# scientific reports

OPEN

# A novel investigation using thermal modeling and optimization of waste pyrolysis reactor using finite element analysis and response surface methodology

Shivi Garg[1], Anand Nayyar[2 ✉], Abdulrajak Buradi[3], Krushna Prasad Shadangi[4], Prabhakar Sharma[5], Bhaskor Jyoti Bora[1], Akshay Jain[1] & Mohd Asif Shah[6,7,8 ✉]

The influence of humans on the environment is growing drastically and is pervasive. If this trend continues for a longer time, it can cost humankind, social and economic challenges. Keeping this situation in mind, renewable energy has paved the way as our saviour. This shift will not only help in reducing pollution but will also provide immense opportunities for the youth to work. This work discusses about various waste management strategies and discusses the pyrolysis process in details. Simulations were done keeping pyrolysis as the base process and by varying parameters like feeds and reactor materials. Different feeds were chosen like Low-Density Polyethylene (LDPE), wheat straw, pinewood, and a mixture of Polystyrene (PS), Polyethylene (PE), and Polypropylene (PP). Different reactor materials were considered namely, stainless steel AISI 202, AISI 302, AISI 304, and AISI 405. AISI stands for American Iron and Steel Institute. AISI is used to signify some standard grades of alloy steel bars. Thermal stress and thermal strain values and temperature contours were obtained using simulation software called Fusion 360. These values were plotted against temperature using graphing software called Origin. It was observed that these values increased with increasing temperature. LDPE got the lowest values for stress and stainless steel AISI 304 came out to be the most feasible material for pyrolysis reactor having the ability to withstand high thermal stresses. RSM was effectively used to generate a robust prognostic model with high efficiency, $R^2$ (0.9924–0.9931), and low RMSE (0.236 to 0.347). Optimization based on desirability identified the operating parameters as 354 °C temperature and LDPE feedstock. The best thermal stress and strain responses at these ideal parameters were 1719.67 MPa and 0.0095, respectively.

**Abbreviations**

| | |
|---|---|
| AISI | American Iron and Steel Institute |
| ANOVA | Analysis of variance |
| BET | Brunauer–Emmett–Teller |
| FEA | Finite element analysis |
| LDPE | Low-density polyethylene |
| PE | Polyethylene |
| PP | Polypropylene |

[1]Energy Institute, Bengaluru, Centre of Rajiv Gandhi Institute of Petroleum Technology, Bangalore, Karnataka 562157, India. [2]Graduate School, Faculty of Information Technology, Duy Tan University, Da Nang 550000, Viet Nam. [3]Department of Mechanical Engineering, Nitte Meenakshi Institute of Technology, Bangalore, Karnataka 560064, India. [4]Department of Chemical Engineering, Veer Surendra Sai University of Technology, Burla, Sambalpur, Odisha 768018, India. [5]Department of Mechanical Engineering, Delhi Skill and Entrepreneurship University, New Delhi 110089, India. [6]Department of Economics, Bakhtar University, Kabul 2496300, Afghanistan. [7]School of Business, Woxsen University, Kamkole, Sadasivpet, Hyderabad, Telangana 502345, India. [8]Division of Research and Development, Lovely Professional University, Phagwara, Punjab 144001, India. ✉email: anandnayyar@duytan.edu.vn; ohaasif@bakhtar.edu.af

| PPP | PS + PP + PE |
|-----|--------------|
| PS | Polystyrene |
| PWS | Pinewood |
| RSM | Response surface methodology |
| $R^2$ | Coefficient of determination |
| WS | Wheat straw |

In recent decades, the application of renewable energy resources is gradually increasing day by day due to the continuous shrinking of fossil fuels and their resources[1,2]. Energy plays a crucial role in any country's economic development[3]. India has a strong influence on the global energy market[4]. In a view of the growing population of India since 2000, the energy demand has increased more than double (Fig. 1). The increasing urbanization and industrialization ensure rise in India's energy demand. There is a huge difference in the energy use pattern across different states and between rural and urban areas. Two factors that are crucial to Indian consumers are affordability and reliability of energy sources[5,6].

Humans have been utilizing a wide variety of biomass resources as a key renewable energy resource for the past many years due to their carbon–neutral content and play a major role in controlling the harms concerning the change of climate as per the climate change information. The advent of fossil fuels, this dependency is somewhat reduced. However, recent increasing transportation fuel demand, over-dependence on fossil fuels, increasing global warming and climate change suggests that efforts should be made to shift our economy towards the renewable sector[7,8]. For a sustainable future, a pollution-free environment, less dependency on fossil fuels and oils, clean air to breathe, and water to drink, humanity needs to move towards the usage of renewable sources available in nature[9–11]. Biomass feedstock is one such useful resource present in nature. Apart from giving a clean and sustainable environment, this has the potential of giving new opportunities to young people[12,13]. Although research is going on this topic and many technologies are already available, still there is a long way to go for the products to be economically accepted and feasible. The social perspectives suggest that a bio-based economy will not only benefit the environment but will also open doors to more employment in the farming and industrial sectors. As seen in the past few years, the renewable sector has achieved significant growth[14,15].

In many countries, biomass resources are not sufficient to satisfy the energy demands and this situation is termed a 'secondary energy crisis'. The problem of rising oil prices goes along with this problem[16]. There is a need to develop ways to utilize renewable energy sources from the countries to mitigate this dual-energy problem. The society must be aware of all the implications that biomass resources might cause, both good and bad. There could be many barriers to the utilization of biomass resources[17] such as infrastructure, financial and other resources, manufacturing knowledge and technological aspects. However, the immense potential of biomass is one encouraging factor in terms of a green economy with subsidiary benefits[18,19].

Recent era has another problem along with the energy crisis is the air pollution caused by the increased usage of plastic materials[20]. Most of the plastic waste is either ends to landfills or incinerated. These processes are harmful for the environment and causes air pollution. Increased dumping of plastics into landfills pollutes the environment which ultimately degrade the ecosystem[21]. The world is surrounded by plastics. From the syringe to the computer, everything is made of plastic. Even the Covid19 protective gear are made of plastic. Due to these applications in today's life, people have become dependent on this one-time-use article. The ways through which plastic can be eliminated are shown in Fig. 2.

Some conventional ways of waste management include open burning or incineration, which leads to pollution of air. The burning of plastic waste releases many toxins such as carbon monoxide, volatile organic compounds, smoke, and polycyclic aromatic hydrocarbons into the air[22]. One of the most advanced techniques to convert waste plastic in to fuel is pyrolysis[23].

Pyrolysis involves the conversion of feedstock into a mixture of oils, gases, and solid charcoal. The application to heat to the feedstock in the absence of oxygen breaks it down into small chain molecules. The pyrolysis process is divided into two phases: The first phase deals with the fragmentation of molecules and depolymerization of polymers into monomers. This phase takes place within a temperature range of 150–300 °C. Free radicals are generated in this stage which leads to the formation of hydroxyl, and carboxyl groups. Free radicals contain
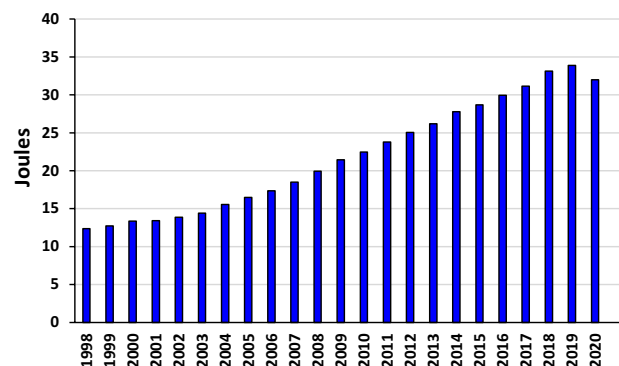


**Figure 1.** India's energy consumption from 1998 to 2020.
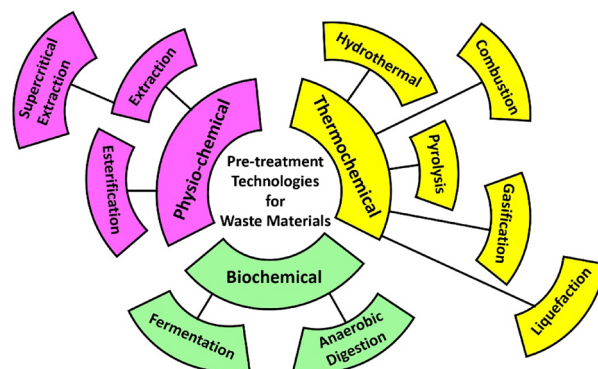
**Figure 2.** Waste material conversion technologies.

lone pairs, which are responsible for the formation of reactive oxygen[24,25]. The second phase executed in the temperature range of 400–600 °C and it includes polymerization, cracking, and condensation. Large molecules tend to deposit on the walls after polymerization which hinders the overall process by reducing the efficiency. By varying different process conditions, pyrolysis oil may be obtained which acts as fuel.

The by-products which are not completely vaporized and consist fixed carbon and ash, which are referred to as char. The problem with the pyrolysis process is that the paralytic oil that we get as the product is thermally unstable due to a large amount of oxygen present in it. Hence, hydrogenation and catalytic cracking of the oil are required to make it thermally stable[26]. Another hurdle with pyrolysis is the generation of flu gas. However, if this gas further treated, then this process can work wonders for the existing problems of plastics and biomass degradation. Pyrolysis is classified based on heating rates as slow pyrolysis or (non-isothermal), in which volatile organic material evaporates partly leaving behind a large part of solid carbon as the main product, called char. Fast pyrolysis or (isothermal) is the one in which feedstock is heated at elevated temperatures within a short span to make pyrolytic oil. The reactor is considered to work isothermally to maximize the product yield. And ultra-flash/flash pyrolysis is an extremely rapid process with a high heating rate and product yield and short residence time[27].

Thermal pyrolysis is a method of depolymerization of materials under very high temperatures in the absence of oxygen. Products include gaseous, liquid, and solid fuel. The condensable volatile fraction forms the liquid fuel, and the remaining non-condensable part is a high calorific value gas. Product properties vary significantly with the type of feedstock. In microwave-assisted pyrolysis[28] the wavelength of microwave radiation ranges from one millimetre to one meter and its frequency ranges from 300 MHz to 30 GHz. Microwave heating is mainly used for instantaneous starting and stopping and for generating rapid heating, which results in higher yields and selectivity of the compounds. Residence time, moisture content, temperature rate, and concentration of microwave absorber are the factors that play a crucial role in determining product quality. High temperature and residence time with low heating rates favor high gas production. In the case of solar pyrolysis, the heat is provided by concentrated solar radiation[29]. Compounds crack into smaller fractions in the primary stage having a temperature range of around 250–500 °C.

In the second stage primary heavy compounds further, crack into smaller molecules at a temperature of 700 °C. In slow pyrolysis, the main product is char because of low temperatures, slow heating rates, and high residence time, while in fast pyrolysis the main product is liquid fuel owing to high temperatures, high heating rates, and low residence time. The main product of solar pyrolysis is a liquid fuel, which means it follows fast pyrolysis[30]. The most common type of reactor used here is a direct heating reactor in which there is one glass window and a concentrator in the reactor to focus the concentrated radiation on the feedstock. This method proves to be a better alternative in terms of heat and efficiency. There is one indirect heating method also, but due to high heat losses and complicated heat transfer circuits, it is not at all preferred.

**Objectives of paper.** The following are the objectives of paper:

- To conduct the examination of thermal stress and thermal strain experienced by the pyrolysis reactor as a result of high temperatures and pressures. In this regard, four different materials of the reactor along with four different feedstocks are considered. The simulation study for determination thermal stress and thermal strain is carried out Fusion 360 simulation software.
- To perform modeling and optimization of thermal stress and thermal strain for different feeds and reactor materials of the pyrolysis process through Response Surface Methodology.

**Organization of paper.** "Literature review" section highlights literature review that reveals previous work related to the current topic. "Materials and methods" section discusses the materials and methods used in the investigation, as well as the subsequent optimization and numerical approaches. The results are then given and discussed in "Results and discussion" section. "Conclusion and future scope" section concludes the paper with future scope.

## Literature review

Various experimental and computational investigations highlighted the effect of multiple parameters on pyrolysis. In this regard, Wang et al.[30] tested with different pyrolysis temperatures, feed rates of rice straw and Camellia oleifera shell using microwave radiation as the heating source. The outcome of the study was reported that the yield of bio-oil increased with an increase in temperature in the case of rice straw while it decreased with an increase in temperature in the case of camellia oleifera. However, the pyrolytic oil/bio-oil that we get from thermal pyrolysis requires a high-temperature range and retention time. Also, the quality of the oil was less. These issues can be rectified by using a catalyst. Shadangi et al.[31] studied thermal and catalytic pyrolysis of Karanja oil seeds. The experiment was performed in a semi-batch reactor and aimed at finding out the optimum temperature for pyrolysis. CaO, Kaolin, and $Al_2O_3$ were used as catalysts in different ratios with the feed. Composition analysis revealed that the pyrolytic oil produced through catalytic pyrolysis had a higher calorific value as compared to the pyrolytic oil produced from thermal pyrolysis. Das et al.[32] analyzed the samples of LDPE, High-Density Polyethylene, and PP at a slow dynamic condition. It was reported that the pyrolysis temperature played an important role in determining the composition of the pyrolytic oil. Also, the concentration of paraffin increased with increasing temperatures while the concentration of olefin decreased. In a study reported by Barbarias et al.[33], a mixture of PS, PE, PP, and polyethylene terephthalate was assessed for pyrolysis. The process was divided into two parts, the first being the pyrolysis step and the other reforming step. The products were analysed by gas chromatography and micro-gas chromatography. For the catalytic process to work efficiently, the perfect choice of the reactor is required. Various types of reactors have been proposed Shadangi et al.[31] for pyrolysis in the literature for commercial use. The most common type of reactor is the fluidized bed reactor which is mainly preferred for the catalytic processes. These reactors are flexible to various feeds and have got high heat and mass transfer rates. It was concluded that high heating rates were due to the proper mixing of biomass material with the bed material. The reactor material plays an important role in handling high heat and pressure. Stainless steel is the most widely used reactor material for pyrolysis due to its corrosion-resistant properties. Moreover, it can withstand high temperatures and pressure as reported by a few studies[34,35]. The simulation study done by Sadhukhan et al.[36] consisted of analyzing the effects of temperature and particle size. A mathematical model was formulated, and it was solved using the Finite Volume Method with Tri-Diagonal Matrix Algorithm approach. The model was further verified by the experimental results.

The thermal stress–strain behavior of the pyrolysis reactor's body is critical, yet it is a complicated process. Its modeling with first principles is difficult and fraught with ambiguity. However, modern machine learning techniques, paired with faster computing power, give a foundation for developing parametric modeling and optimization[37]. This is a more realistic approach to modeling engineering problems and systems. It employs analysis of variance (ANOVA) on data gained via experimental research. The response surface methodology (RSM) has been used in recent times in various engineering fields such as biofuel research[38], dual-fuel combustion[39], emission modeling[40], and nanofluids characterization[41] among others. Several authors have employed RSM to optimize the operating parameters of pyrolysis reactors to optimize their output. Das and Goud[42] employed RSM to maximize bio-oil output. A quadratic model based on ANOVA was built to analyze the trend and connection between the test responses and the process parameters, namely nitrogen mass flow rate (0.87–1.5 LPM), temperature (300–600 °C), and holding duration (20–60 min). The temperature had the greatest impact, followed by holding duration and nitrogen flow rate. In another study, Tripathi et al.[43] employed RSM to improve the output of oil palm shell-based char and Brunauer–Emmett–Teller (BET) surface area by optimizing process parameters. The operating parameters for maximizing OPS char production (60.93%) and BET surface area (250.03 m²/g) were determined using the ANOVA analysis of the experimental data. The anticipated findings were confirmed, and it was discovered that the experimental data differed from the projected values by only 5.99% in yield and 6.34% in BET surface area.

The literature review indicates that there has not been enough research done on the behaviour of different feeds in terms of thermal stress and thermal strain values. Also, the effect of different reactor materials has not been touched upon yet. Another significant research gap is the non-availability of modeling-optimization studies in this domain. According to the literature review, even though RSM is a rigorous modeling-optimization approach, its potential use in the pyrolysis reactor's thermal stress–strain paradigm for modeling prediction has not been examined.

## Materials and methods

**Software analysis.** Fusion 360 simulation software was used for doing a 3D analysis of the pyrolysis reactor based on different feedstock and different reactor materials. This software gives us the steady state analysis while taking into account the heat flow. Hence, atleast one heat load is required to simulate the heat flow. Also, the thermal conductance in this software takes the value infinity by default, if not stated otherwise. While doing this analysis, meshing was performed on the reactor for Finite Element Analysis (FEA). Fusion 360 works on the principle of the Finite Element approach. Table 1 shows the materials which were considered in this study. One feed was selected at a time and its thermal and structural analysis was done. The thermal analysis gave the temperature profile for that particular feed and that profile was further used to get the thermal stress and strain values. Figures 3, 4, 5 and 6 show meshing refinement which was done to get accurate results and to minimize the error. The dimension of the Pyrolyser is referred from a previous study[44].

### Governing equations behind fusion 360 software.

- Thermal analysis of the pyrolysis reactor is based on the Heat Transfer concepts of conduction and convection (Assumption 1).

| Feeds | Reactor materials |
|---|---|
| LDPE | Stainless steel AISI 202 |
| Wheat straw | Stainless steel AISI 302 |
| Pinewood | Stainless steel AISI 304 |
| PS + PE+PP | Stainless steel AISI 405 |

**Table 1.** Computational matrix.



**Figure 3.** Meshing with element size of 100 mm.



**Figure 4.** Meshing with element size of 50 mm.

- Conduction is used while studying the temperature profile throughout the reactor, whereas convection helps to understand the heat transfer from the reactor body to the surroundings (Assumption 2).
- Thermal analyses are steady-state heat transfer analyses used to determine the steady-state temperature distribution and heat flow (Assumption 3).
- The thermal conductivity of the material must be known as well as the ambient temperature and heat transfer coefficients at convection (Assumption 4).

**Figure 5.** Meshing with element size of 30 mm.



**Figure 6.** Meshing with element size of 20 mm.

- Heat is always transferred in the direction of decreasing temperature (Assumption 5).

  Following equations are used to show these concepts:

1. Heat Transfer:

$$Q = mc\Delta T,\qquad(1)$$

where m = mass of the system, c = Specific heat of the system, $\Delta T$ = Change in temperature of the system, Q = Heat transferred.

2. General Conduction:

$$\text{Fourier's law, , } Q = -k\,A\,\frac{dT}{dx},\qquad(2)$$

where k = Thermal conductivity of the material, A = Area of the surface, $\frac{dT}{dx}$ = Temperature gradient.

3. Convection:

$$Newton's\ law\ of\ cooling,\ Q\ =\ hA\ \Delta T, \tag{3}$$

where h = Heat transfer coefficient of the material, A = Area of the surface, $\Delta T$ = Temperature difference between surface and surroundings.

- Structural analysis is explained using the concept of coefficient of thermal expansion, which results in generating stresses throughout the reactor body.
- Volumetric thermal expansion, $\beta$ is used to explain the expansion of the reactor.
- The outer diameter of the reactor after the expansion can be calculated as follows:

$$D_1\ =\ D_0(1+\ \beta T), \tag{4}$$

where $D_1$ = diameter after expansion, $D_0$ = diameter before expansion.

**Mesh independence test.** In an FEA model, the geometry is divided into a series of discrete points called nodes. This process is called meshing. Too many nodes indicate more computation time and a smaller number of nodes indicate inaccurate results. Hence, to come to an accurate solution, an optimized number of nodes should be chosen so that the results are independent of the mesh size. This process is called convergence. Mesh convergence ensures accurate results. Table 2[22,42,44] shows different pyrolysis range based on which contours were generated for other feeds as well. It was observed that the thermal stress and strain values increased with increasing temperatures.

Figure 7 depicts Mesh Independence Test which was performed to do the error analysis. The arrow in this figure points to one small horizontal line which shows that the results have reached a constant point and the value of the thermal stress is not changing with mesh size anymore.

**Model validation.** For the same design, same boundary conditions and turbulence models, the results obtained from the present model using Fusion 360 simulation software is compared the previous model of Jha et al.[42] designed for biomass pyrolysis reactor. Figure 8 indicates that the present work follows a similar trend to that Jha et al.[42] which validates the model.

**Response surface methodology.** The RSM can establish the settings of the input variables and optimize a single or a series of outputs. Also, within certain constraints, RSM optimizes the optimal output responses by maximizing or decreasing process parameters. RSM was used in this work to create a predictive model that consists of a set of quadratic algebraic equations. The data collected during the experimental phase was used for the modeling. The second-degree polynomial expression denotes the RSM-based model:

| Feeds | Pyrolysis range |
|---|---|
| LDPE | 410–465 |
| Wheat straw | 20–600 |
| Pinewood | 20–470 |
| PE+PS + PP | 20–500 |

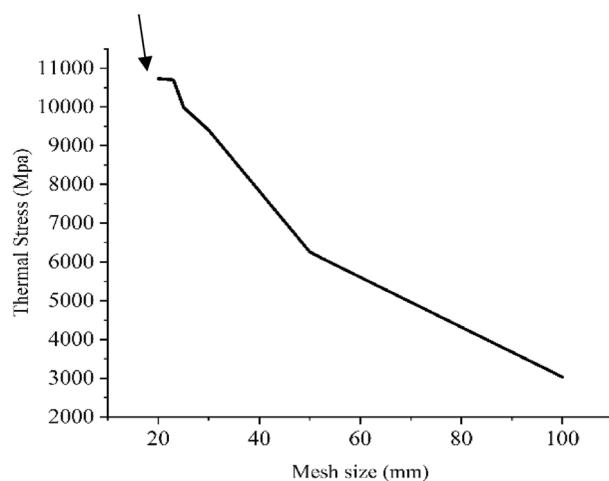**Table 2.** Pyrolysis range of feeds[22,42,44].
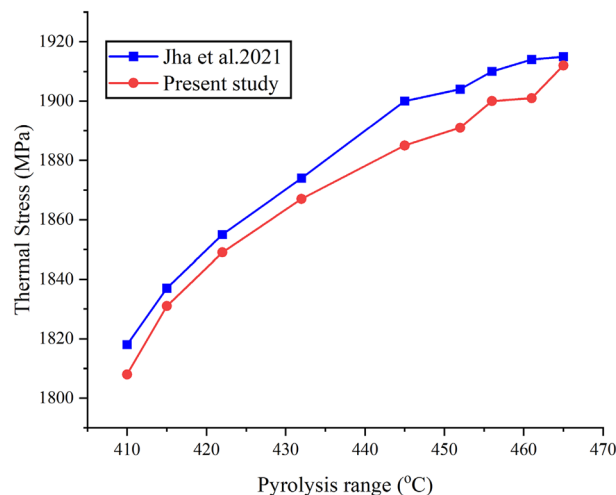


**Figure 7.** Mesh independence test.

**Figure 8.** Model validation.

$$y = d_0 + \sum_{n=1}^{k} d_i x_i + \sum_{i=1}^{k} \sum_{j \geq i}^{k} d_{ij} x_i x_j + \epsilon. \tag{5}$$

Herein, $y$ denotes the forecasted response while $d_0$ represents bias. The $i$ and $j$ denote coefficients for a linear and quadratic function. The $d_i$ and $d_{ij}$ are linear and interactive coefficients, k is the number of components, $x_i$ and $x_j$ are independent variables, and $\epsilon$ is the random error identified in the response. The RSM-based model was evaluated based on statistical measures such as coefficient of determination ($R^2$), the predicted $R^2$, and the adjusted $R^2$. The desirability technique was utilized to do parameterized optimization to get the best outcome. The optimization investigation was carried out using Design-Expert software, which translates each response to a dimensionless desire value (), that may be obtained in the band of 0 to 1. The zero values indicate an undesirable reaction, whereas the value = 1 indicates a highly desired response. Based on the problem at hand, the objective of any solution might be to accomplish a maximum, a decrease, a target, to remain within a range, or to be equal to. The flow chart of the optimization process employed in the present study is shown in Fig. 9.

**Data collection and pre-processing.** Thermal stress and strain developed during the pyrolysis of different biomass feeds and at different temperatures were modelled using ANOVA. The historical data approach was used to build the model. This software assumes that the observations are mutually independent to each other and normally distributed. These assumptions suggest that the output of one investigation should not hamper the output of the other investigation or observation. The experimental design consisted of 27 runs and 108 data points (4 parameters 27 runs). Table 3 displays the experimental research data as a designed array.

The quality of the data is quite a significant factor in the development of a strong machine learning model. The current research comprised two inputs (one categorical and one numerical) i.e., type of feed and temperature. There were two outputs namely thermal stress and thermal strain. In all, twenty-seven data sets were gathered through experimentation. Descriptive statistics were employed to highlight the nature and symmetry of the data. The findings of descriptive statistics are shown in Table 4. Descriptive statistics is also highly essential since it would be difficult to picture what the data was indicating if we just presented it as raw data. Positive skewness indicates that the probability density function's left side is bigger than its right side. In other words, there are fewer high-value data points than low-value data points. A negative skewness value may also be seen. Table 4 shows that the majority of the output results data has a skewness of zero or very near to zero, suggesting a normal distribution. Kurtosis is a statistical concept that compares the form of the data distribution to that of the normal distribution. Kurtosis is 0 for a normal distribution, while it is negative for a flatter distribution and positive for a more peaks distribution. Values close to 0 (Table 4) suggest a normal distribution in the current circumstances. The data was subsequently submitted to outlier and nil data tests; however, no outliers or missing values were found.

**ANOVA and development of correlation functions.** ANOVA, a statistical method used to determine if the mean of two groups varied, was utilized in the present investigation. The deductive approach employs sample analysis to derive population characteristics. ANOVA assists us in determining if the sample results are relevant to populations. The p-value of the ANOVA result may be used to assess if there are statistically significant differences between some of the means. The p-value of the data was compared to a predetermined significance threshold to assess if the mean differences are statistically significant. To assess variance between groups, the F-index was estimated. A higher F-index indicates that the deviations among groups are greater than the variance within the groups. In such instances, the means of the groups are more likely to deviate.
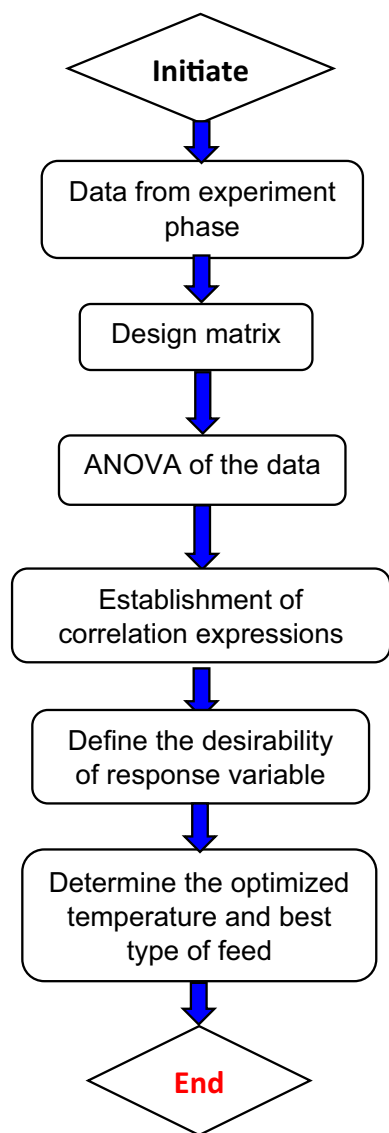
**Figure 9.** Flow chart of optimization process.

The ANOVA results are shown in Table 5. The F-index of 3.176E+007 for the thermal stress model and 1.574E+007 for the thermal strain model indicates that it was significant enough to merit examination. It also shows that there is a 0.01% chance that such a high F-index is due to noise. The model terms are significant if the p-value is less than 0.0500. For both thermal stresses as well as thermal strain models, the model variables T, B, and TB were significant.

## Results and discussion
**Effect of various feeds.**     Figures 10, 11, 12 and 13 show the variation of different feeds with pyrolysis temperature. Figure 10 shows LDPE thermal stress curve and temperature contour while Fig. 11 shows the same parameters for wheat straw. Figure 11 depicts the thermal stress and temperature contour of pinewood while Fig. 12 shows the same values for the PS + PE + PP mixture. Based on these results, it was concluded that the thermal stress and strain values increase with increasing temperatures. LDPE got the least thermal stress and strain values, and wheat straw got the highest values.

Figures 14, 15, 16 and 17 show the behavior of different reactor materials with various feeds (having different pyrolysis temperatures). It was observed that Stainless steel AISI 304 could withstand high temperatures and pressures due to the presence of high chromium and nickel content in it.

**Modeling and optimization.**     The RSM-based models developed in the form of mathematical equations as shown in "Modeling and optimization" section (Eqs. 6–13) were used to predict the model output for different feedstocks and temperatures. The performance of these models and parametric optimization is discussed in the following sections.

| Test run | Temperature (°C) | Type of feed | Thermal stress (MPa; Von Mises) | Thermal strain (Equivalent) |
|---|---|---|---|---|
| 1 | 410 | LDPE | 1814 | 0.01099 |
| 2 | 415 | LDPE | 1822 | 0.01112 |
| 3 | 422 | LDPE | 1834 | 0.0113 |
| 4 | 431 | LDPE | 1849 | 0.01154 |
| 5 | 445 | LDPE | 1873 | 0.01191 |
| 6 | 452 | LDPE | 1885 | 0.0121 |
| 7 | 458 | LDPE | 1895 | 0.01225 |
| 8 | 462 | LDPE | 1901 | 0.01236 |
| 9 | 465 | LDPE | 1907 | 0.01244 |
| 10 | 20 | WS | 0.00045 | 3.3E-009 |
| 11 | 125 | WS | 626.2 | 0.00408 |
| 12 | 250 | WS | 1372 | 0.00894 |
| 13 | 375 | WS | 2117 | 0.01381 |
| 14 | 500 | WS | 2863 | 0.01867 |
| 15 | 600 | WS | 3459 | 0.02256 |
| 16 | 20 | PWS | 0.00045 | 3.3E-009 |
| 17 | 100 | PWS | 477.1 | 0.00311 |
| 18 | 200 | PWS | 1074 | 0.007 |
| 19 | 300 | PWS | 1670 | 0.01089 |
| 20 | 400 | PWS | 2266 | 0.01478 |
| 21 | 470 | PWS | 2684 | 0.0175 |
| 22 | 20 | PPP | 0.00045 | 3.3E-009 |
| 23 | 116 | PPP | 572.6 | 0.00373 |
| 24 | 212 | PPP | 1145 | 0.007467 |
| 25 | 308 | PPP | 1718 | 0.0112 |
| 26 | 404 | PPP | 2290 | 0.01493 |
| 27 | 500 | PPP | 2863 | 0.01867 |

**Table 3.** Design array.

| Particulars | Temp. (°C) | Thermal stress (MPa; Von Mises) | Thermal strain (Equation) |
|---|---|---|---|
| Mean | 328.8 | 1628.8 | 0.0104 |
| Standard error | 32.52 | 173.47 | 0.0011 |
| Median | 404 | 1834 | 0.0113 |
| Standard deviation | 169.01 | 901.37 | 0.0058 |
| Sample variance | 28,566.49 | 812,483.8 | 3.43−05 |
| Kurtosis | −0.794 | −0.235 | −0.209 |
| Skewness | −0.650 | −0.290 | −0.226 |
| Range | 580 | 3459 | 0.022 |
| Maximum | 600 | 3459 | 0.022 |
| Minimum | 20 | 0.00045 | 3.3E−09 |
| Sum | 8880 | 43,976.9 | 0.2833 |
| Count | 27 | 27 | 27 |

**Table 4.** Descriptive statistical analysis of the data.

| Particulars | Thermal stress model | | Thermal strain model | | |
|---|---|---|---|---|---|
| | F-index | p-value | F-index | p-value | |
| Model | 3.176E+007 | < 0.0001 | 1.574E+007 | < 0.0001 | Significant |
| Temp | 2.384E+008 | < 0.0001 | 1.198E+008 | < 0.0001 | |
| Feed type (B) | 7.497E+006 | < 0.0001 | 4.476E+006 | < 0.0001 | |
| TB | 2.506E+005 | < 0.0001 | 25,257.22 | < 0.0001 | |
| $T^2$ | 0.18 | 0.6733 | 1.14 | 0.2991 | |

**Table 5.** ANOVA results. *T* temperature term, *B* type of feed supplied.
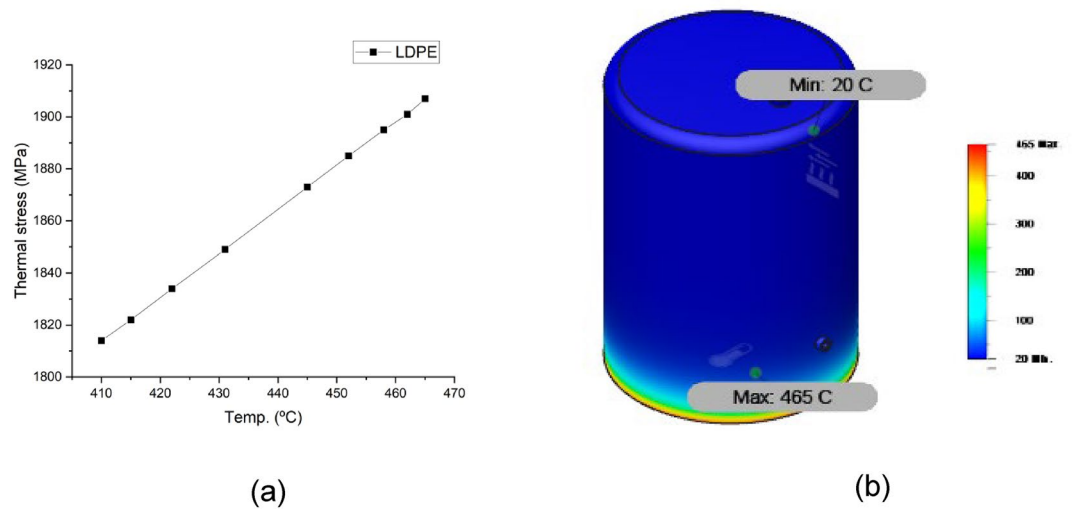
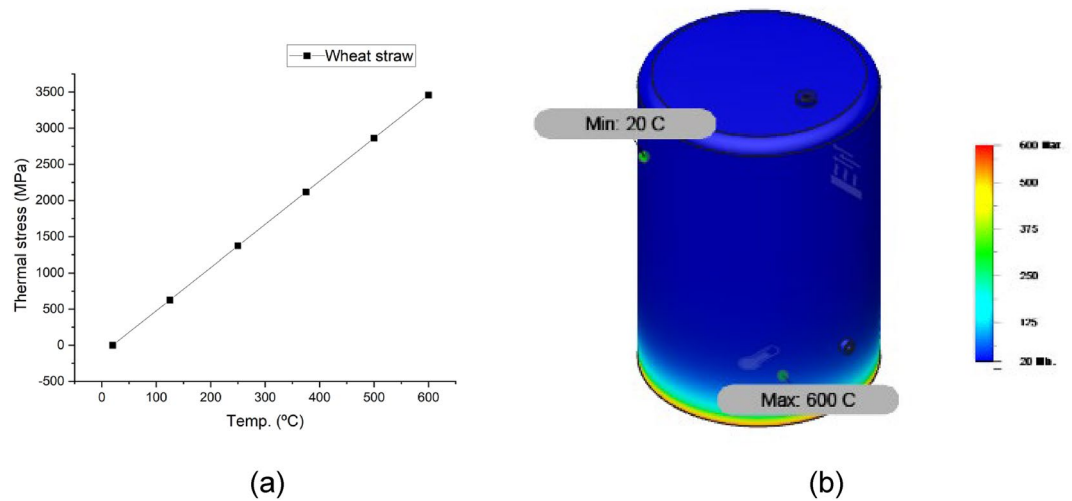**Figure 10.** LDPE (**a**) thermal stress curve, (**b**) temperature contour.



**Figure 11.** Wheat straw (**a**) thermal stress curve, (**b**) temperature contour.
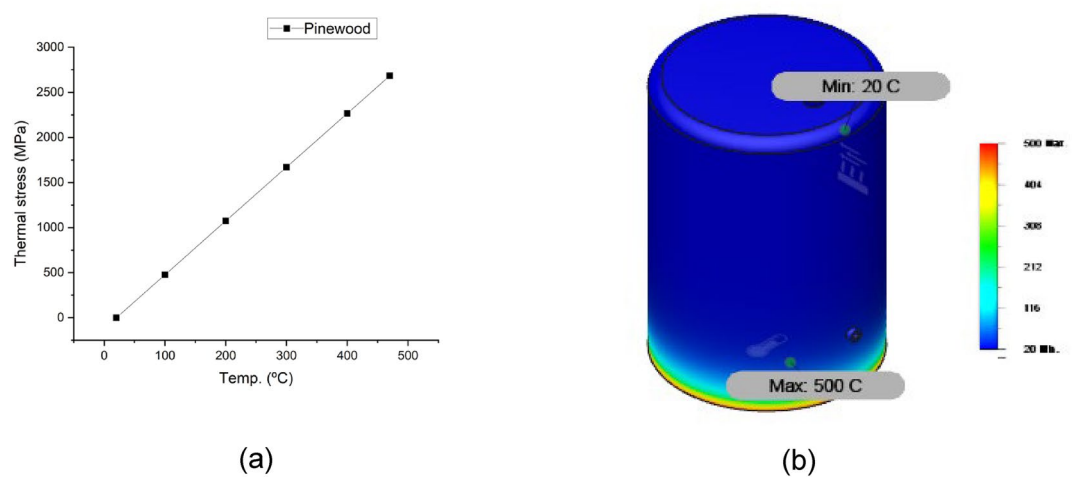


**Figure 12.** Pinewood (**a**) thermal stress curve, (**b**) temperature contour.
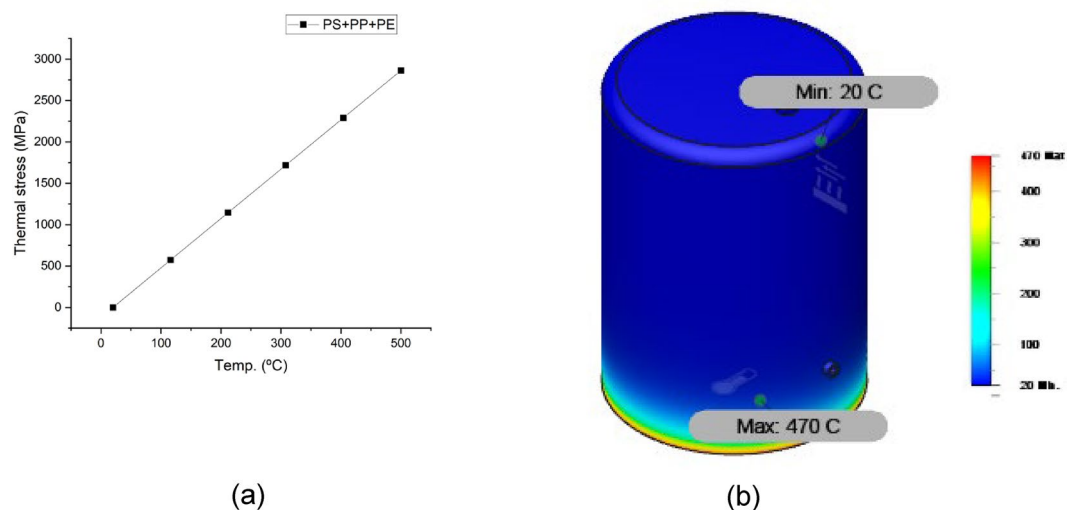
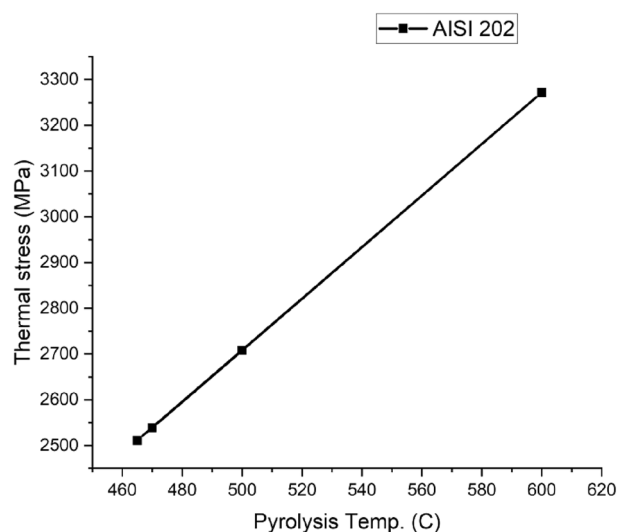**Figure 13.** PS + PE + PP (**a**) thermal stress curve, (**b**) temperature contour.



**Figure 14.** AISI 202 Thermal stress curves.

The ANOVA of the data also helped in deducing the correlation between independent control factors (temperature and type of feed) and response variables (thermal stress and strain). The algebraic expression developed for thermal stress caused by different types of feeds is shown below in Eqs. (6) to (9):

Feed type: LDPE

$$Thermal\ stress = 1120.64 + 1.69T - 1.12E - 006 \times T^2. \qquad (6)$$

Feed type: WS

$$Thermal\ stress = -119.3 + 5.97T - 1.126E - 006 \times T^2. \qquad (7)$$

Feed type: PWS

$$Thermal\ stress = -119.22 + 5.97T - 1.126E - 006 \times T^2. \qquad (8)$$

Feed type: PPP

$$Thermal\ stress = -119.34 + 5.97T - 1.127E - 006 \times T^2. \qquad (9)$$

The correlation developed for thermal strain due to different type of feeds are shown below in Eqs. (10) to (13):

Feed type: LDPE
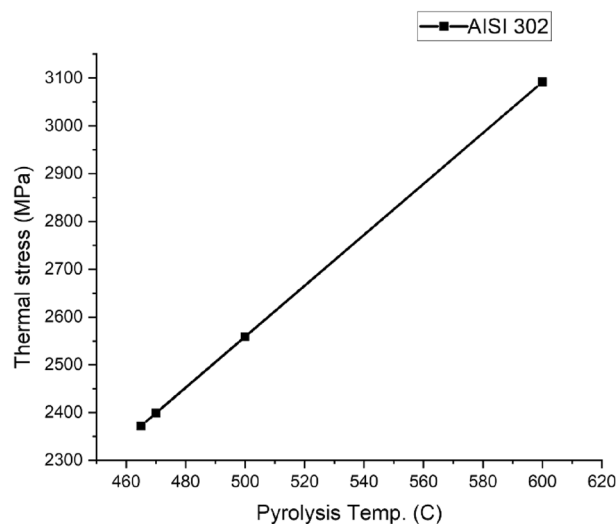
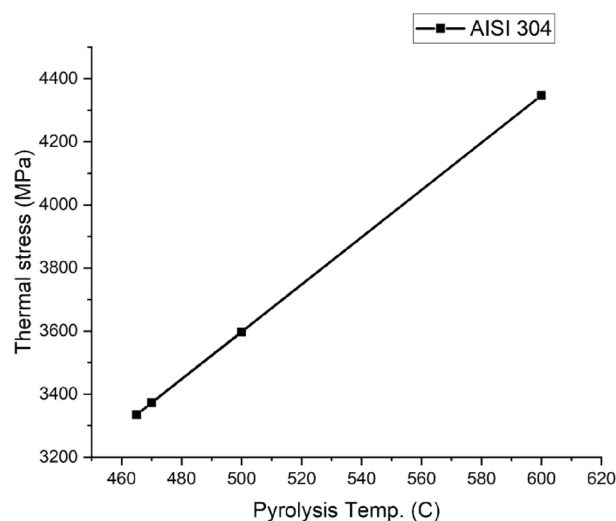**Figure 15.** AISI 302 Thermal stress curve.



**Figure 16.** AISI 304 Thermal stress curve.

$$Thermal\ strain = 1.72E - 004 + 2.64E - 005T + 2.59E - 011 \times T^2. \tag{10}$$

Feed type: WS

$$Thermal\ strain = -7.79E - 004 + 3.89E - 005T + 2.59E - 011 \times T^2. \tag{11}$$

Feed type: PWS

$$Thermal\ strain = -7.78E - 004 + 3.89E - 005T + 2.59 - 011 \times T^2. \tag{12}$$

Feed type: PPP

$$Thermal\ strain = -7.77E - 004 + 3.88E - 005T + 2.6E - 011 \times T^2. \tag{13}$$

*Thermal stress model.*    Equations (6) to (9) were utilized to predict the outcomes (thermal stress) for all four types of pyrolysis feeds at the whole range of operational parameters. Table 6 shows how the findings were utilized to construct several statistical indices for model assessment. Figure 18a depicts a graphical comparison of observed and forecasted thermal stress developed in the metallic body of the reactor body, whereas Fig. 18b shows a graph of studentized residuals in the model predicted values. The graphical representation of compari-son model values and low residuals in Fig. 18a,b shows that the RSM-based developed model was a robust prog-nostic model. The statistical examination of the results, as shown in Table 6, corroborated this conclusion. The
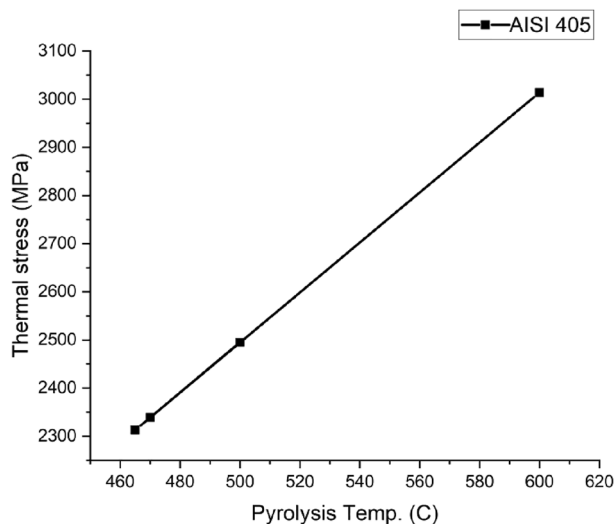
**Figure 17.** AISI 405 Thermal stress curve.

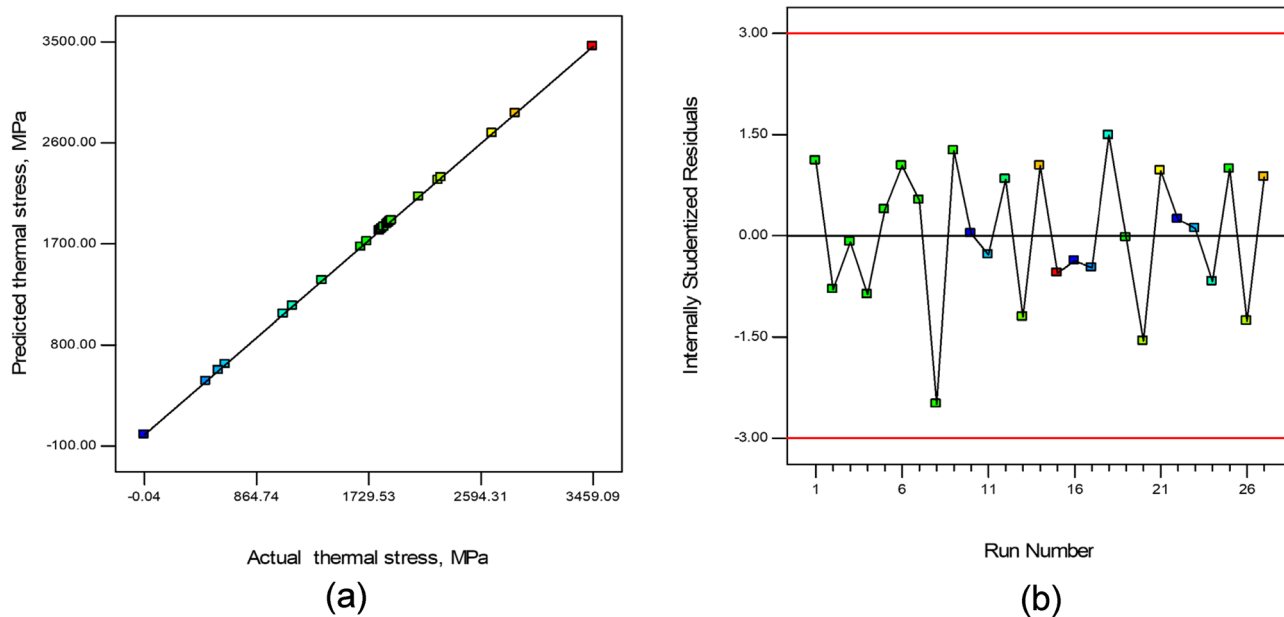| | R² | R² (Adjusted) | R² (Predicted) | Root mean squared error |
|---|---|---|---|---|
| Thermal stress model | 0.9931 | 0.9914 | 0.9902 | 0.236 |
| Thermal strain model | 0.9924 | 0.9905 | 0.9898 | 0.347 |

**Table 6.** Statistical evaluation of model's performance.



**Figure 18.** Thermal stress (**a**) Actual vs model predicted values, (**b**) Internally studentized residuals.

created model produced a low root mean squared error (RMSE) of 0.236, close to unity values of $R^2$ as 0.9931, $R^2$ (Adjusted) as 0.9902, and $R^2$ (Predicted) as 0.9902, indicating an efficient prediction model for thermal stress.

*Thermal strain model.* The thermal strain models as expressed with Eqs. (10)–(13), being used to estimate the results for all four types of pyrolysis feeds throughout the whole range of operating parameters. Figure 19a displays a graphical comparison of observed and expected thermal strains in the metallic body of the reactor body, while Fig. 19b provides a graph of studentized residuals in the model predicted values. Figure 19a,b displays a
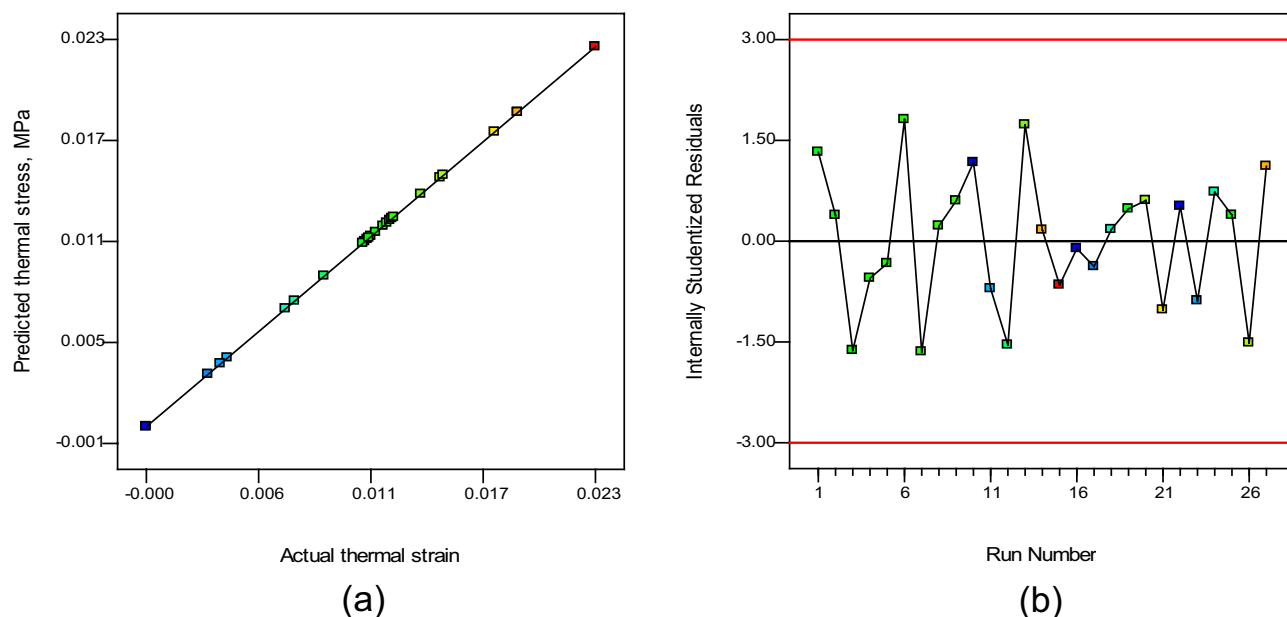
**Figure 19.** Thermal strain (**a**) actual vs model predicted values, (**b**) internally studentized residuals.

graphical depiction of comparison model values and low residuals, indicating that the RSM-based created model was a robust prognostic model. This model conclusion was supported by a statistical assessment of the findings, as shown in Table 6. The developed model provided a low root mean squared error (RMSE) of 0.347, near to unity values of $R^2$ as 0.9924, $R^2$ (Adjusted) as 0.9905, and $R^2$ (Predicted) as 0.9898, demonstrating an effective thermal stress prediction model.

*Desirability based optimization.* The findings of RSM-based model prediction demonstrated a considerable variation in output response throughout the temperature range and also with the type of feed supplied for pyrolysis. Since the optimal thermal stress–strain paradigm needs a trade-off between control elements, a desirability-based method was used to determine the best operating parameters and feedstock. Table 7 describes the conditions for such an optimization, such as the lower and upper boundaries and the goal provided for each solution. Figure 20a displays a desirability diagram showing the trade-off between different control factors, with a bar graph displaying individual and combined desirability. The option with the highest desire index (0.55) was chosen. The best control factors were revealed at 354 °C with LDPE as the feedstock, as shown in Table 7. At these optimal settings, the best thermal stress and strain responses were 1719.67 MPa (Fig. 20b) and 0.0095 (Fig. 20c), respectively.

## Conclusion and future scope

It was concluded that pyrolysis is the panacea for the existing waste management issue. Keeping this vista in mind, a study was conducted on the structural analysis of pyrolysis reactors due to high temperatures and pressures. Fusion 360 was used for the investigation. Four feeds (namely, LDPE, wheat straw, pinewood, and a combination of PS, PE, and PP) and four reactor materials (materials Stainless steel AISI 202, Stainless steel AISI 302, Stainless steel AISI 304, and Stainless steel AISI 202) were considered for the analysis. Based on the study, the following results can be concluded:

- The thermal stress and strain values of the pyrolysis reactor increase with increasing temperatures as seen from the simulation results.
- Amongst the 4 feeds studied in this paper, LDPE comes out to be the most effective feed based on low pyrolysis temperature and low-stress values. Low-stress values favor the process as the reactor deformation is less and therefore, it can withstand more heat.

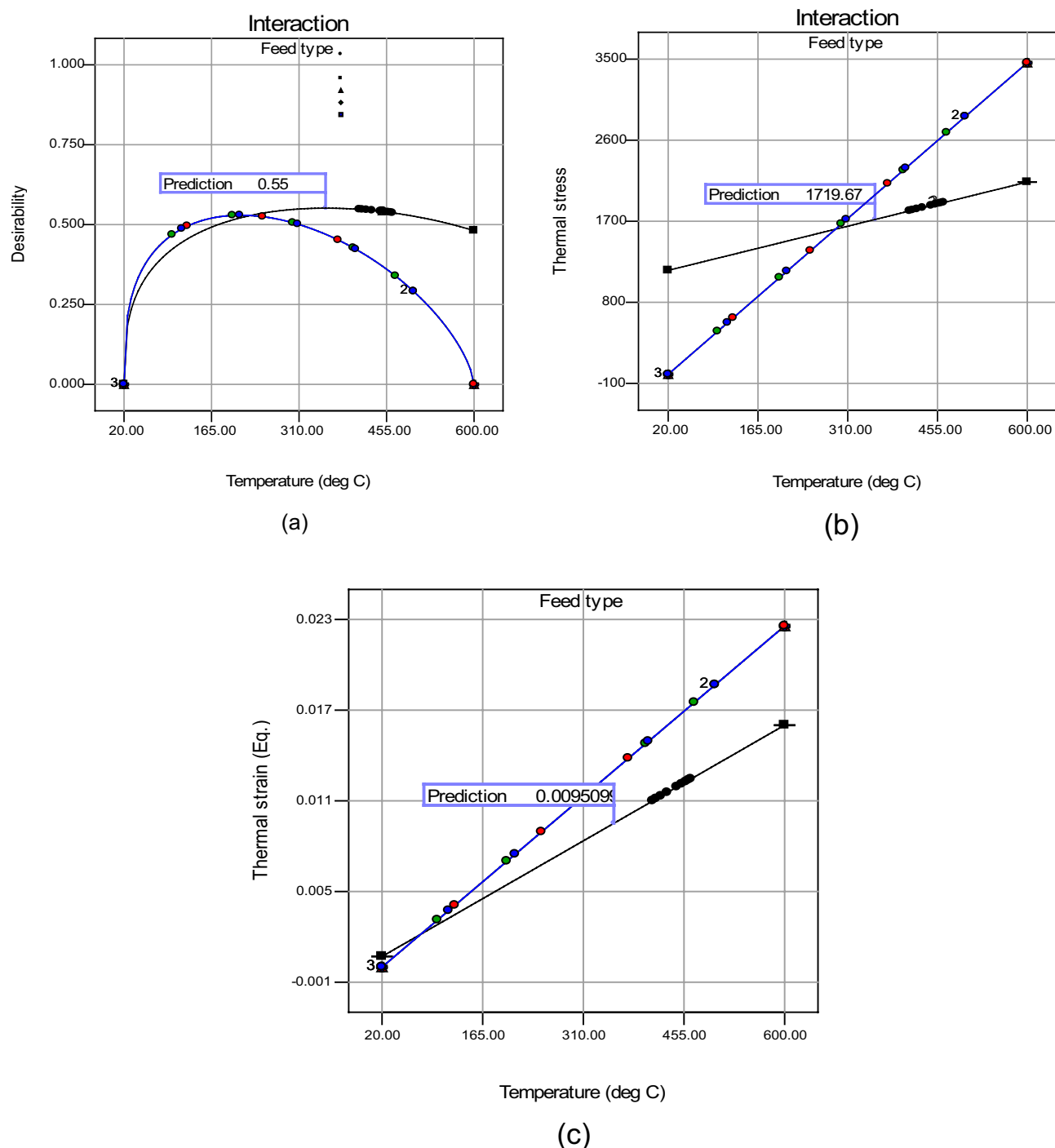| Optimized input factors | | Response variable | |
|---|---|---|---|
| Temperature (°C) | Type of feed | Thermal stress | Thermal strain |
| 354 | LDPE | 1719.67 | 0.0095 |

**Table 7.** Optimization results.

**Figure 20.** Prediction map of (**a**) Desirability, (**b**) thermal stress, (**c**) thermal strain.

- Out of the different grades of stainless steel discussed in this paper, AISI 304 has the best ability to withstand high temperatures owing to its high chromium content of 18–20% and nickel content of 8–11%. Moreover, it can withstand the highest stress of all.
- RSM was successfully employed for the development of a prognostic efficiency with high efficiency having $R^2$ (0.9924–0.9931) and low RMSE as (0.236 to 0.347).
- Desirability-based optimization revealed the optimized pyrolysis temperature of 354 °C with LDPE as the feedstock. At these optimal settings, the best thermal stress and strain response were 1719.67 MPa and 0.0095, respectively.

This paper gives an insight into the structural and thermal analysis, and Response Surface Methodology (RSM) of the pyrolysis reactor by considering various feeds and reactor materials. Simulations help solve real-world problems efficiently and safely while taking into account all the necessary conditions required for the

process. The reactor considered here is optimized to work at 354 °C, having thermal stress and strain response at 1719.67 MPa and 0.0095, respectively.

**Future scope.** Waste to energy is one method that can implanted to address the energy demand of a nation. In this regard, pyrolysis is one of the methods that can be adopted successfully. In this regard, optimisation of the pyrolysis temperature for different feedstocks like municipal waste, medical waste and agricultural residue can attribute to efficient conversion of waste to energy.

## Data availability

The datasets used and/or analysed during the current study available from the corresponding author on reasonable request.

## References

1. Hong, W. Y. & Rahmat, B. N. N. N. Energy consumption, CO2 emissions and electricity costs of lighting for commercial buildings in Southeast Asia. *Sci. Rep.* **12**, 13805 (2022).
2. Raheem, I. *et al.* Forecasting of energy consumption by G20 countries using an adjacent accumulation grey model. *Sci. Rep.* **12**, 13417 (2022).
3. Hasan, M. M., Rasul, M. G., Khan, M. M., Ashwath, N. & Jahirul, M. I. Energy recovery from municipal solid waste using pyrolysis technology: A review on current status and developments. *Renew. Sustain. Energy Rev.* **145**, 111073 (2021).
4. *Global Energy Review 2021* (International Energy Agency).
5. Chew, K. W. *et al.* Abatement of hazardous materials and biomass waste via pyrolysis and co-pyrolysis for environmental sustainability and circular economy. *Environ. Pollut.* **278**, 116836 (2021).
6. Walker, T. W., Motagamwala, A. H., Dumesic, J. A. & Huber, G. W. Fundamental catalytic challenges to design improved biomass conversion technologies. *J. Catal.* **369**, 518–25 (2019).
7. Sharma, P. & Sharma, A. K. Combustion and thermal performance of dual fuel engine: Influence of controlled producer gas substitution with pilot B20 (WCOME Biodiesel–Diesel) blending. *Lecture Notes Mech. Eng.* **20**, 341–354 (2021).
8. Walker, T. W., Motagamwala, A. H., Dumesic, J. A. & Huber, G. W. Fundamental catalytic challenges to design improved biomass conversion technologies. *J. Catal.* **369**, 518–525 (2019).
9. Beigi, H. M., Gadkari, B. S. & Sadhukhan, J. Osmotically assisted reverse osmosis, simulated to achieve high solute concentrations, at low energy consumption. *Sci. Rep.* **12**, 13741 (2022).
10. Yeh, C.-K. *et al.* Real-time energy consumption and air pollution emission during the transpacific crossing of a container ship. *Sci. Rep.* **12**, 15272 (2022).
11. Tariq, G. *et al.* Influence of green technology, green energy consumption, energy efficiency, trade, economic development and FDI on climate change in South Asia. *Sci. Rep.* **12**, 16376 (2022).
12. Singhania, R. R., Guo, W., de Souza Vendenberghe, L. P., Mannina, G. & Kim, S. H. Bioresource technology for bioenergy, bio-products & environmental sustainability. *Bioresour. Technol.* **347**, 126736 (2022).
13. Thiruselvi, D. *et al.* A critical review on global trends in biogas scenario with its up-gradation techniques for fuel cell and future perspectives. *Int. J. Hydrogen Energy* **46**, 16734–16750 (2021).
14. Silva Neto, J. V. & Gallo, W. L. R. Potential impacts of vinasse biogas replacing fossil oil for power generation, natural gas, and increasing sugarcane energy in Brazil. *Renew. Sustain. Energy Rev.* **135**, 110281 (2021).
15. Sharma, P. Artificial intelligence-based model prediction of biodiesel-fueled engine performance and emission characteristics: A comparative evaluation of gene expression programming and artificial neural network. *Heat Transf.* **50**, 5563–5587 (2021).
16. Hoang, A. T. *et al.* Characteristics of hydrogen production from steam gasification of plant-originated lignocellulosic biomass and its prospects in Vietnam. *Int. J. Hydrogen Energy* **47**, 4394–4425 (2022).
17. Raj, T. *et al.* Recent advances in commercial biorefineries for lignocellulosic ethanol production: Current status, challenges and future perspectives. *Bioresour. Technol.* **344**, 126292 (2022).
18. Das, S., Kashyap, D., Kalita, P., Kulkarni, V. & Itaya, Y. Clean gaseous fuel application in diesel engine: A sustainable option for rural electrification in India. *Renew. Sustain. Energy Rev.* https://doi.org/10.1016/j.rser.2019.109485 (2020).
19. Das, S., Kashyap, D., Bora, B. J., Kalita, P. & Kulkarni, V. Thermo-economic optimization of a biogas-diesel dual fuel engine as remote power generating unit using response surface methodology. *Thermal Sci. Eng. Prog.* **24**, 100935 (2021).
20. Kim, S. *et al.* The valorization of food waste via pyrolysis. *J. Clean Prod.* **259**, 120816 (2020).
21. Abraham, A., Park, H., Choi, O. & Sang, B. I. Anaerobic co-digestion of bioplastics as a sustainable mode of waste management with improved energy production—A review. *Bioresour. Technol.* **322**, 124537 (2021).
22. Quesada, L., Calero, M., Ángeles Martín-Lara, M., Pérez, A. & Blázquez, G. Production of an alternative fuel by pyrolysis of plastic wastes mixtures. *Energy Fuels* **34**, 1781–1790 (2020).
23. Das, A. K., Panda, A. K. & Hansdah, D. *Renewable Energy and Its Innovative Technologies. Renewable Energy and its Innovative Technologies* (Springer, 2018).
24. Chen, W. H. *et al.* A comprehensive analysis of food waste derived liquefaction bio-oil properties for industrial application. *Appl. Energy* **237**, 283–291 (2019).
25. Kirubakaran, V. *et al.* A review on gasification of biomass. *Renew. Sustain. Energy Rev.* **13**, 179–186 (2009).
26. Primaz, C. T., Ribes-Greus, A. & Jacques, R. A. Valorization of cotton residues for production of bio-oil and engineered biochar. *Energy* **235**, 121363 (2021).
27. Reed, T. B. Principles and technology of biomass gasification. *Adv. Sol Energy Annu. Rev. Res. Dev.* **2**, 125–174 (1985).
28. Ethaib, S. *et al.* Processes microwave-assisted pyrolysis of biomass waste: A mini review. *Processes* **8**, 1190. https://doi.org/10.3390/pr8091190 (2020).
29. Rahman, M. A., Parvej, A. M. & Aziz, M. A. Concentrating technologies with reactor integration and effect of process variables on solar assisted pyrolysis: A critical review. *Thermal Sci. Eng. Prog.* **25**, 100957 (2021).
30. Wang, Y. *et al.* Production of bio-oil from agricultural waste by using a continuous fast microwave pyrolysis system. *Bioresour. Technol.* **269**, 162–168 (2018).
31. Shadangi, K. P. & Mohanty, K. Thermal and catalytic pyrolysis of Karanja seed to produce liquid fuel. *Fuel* **115**, 434–442 (2014).
32. Das, P. & Tiwari, P. The effect of slow pyrolysis on the conversion of packaging waste plastics (PE and PP) into fuel. *Waste Manag.* **79**, 615–624 (2018).
33. Barbarias, I. *et al.* Valorisation of different waste plastics by pyrolysis and in-line catalytic steam reforming for hydrogen production. *Energy Convers. Manag.* **156**, 575–584 (2018).

34. Schweitzer, D. *et al.* Pilot-scale demonstration of oxy-SER steam gasification: Production of syngas with pre-combustion CO2 capture. *Energy Procedia* **86**, 56–68 (2016).
35. George, J., Arun, P. & Muraleedharan, C. Assessment of producer gas composition in air gasification of biomass using artificial neural network model. *Int. J. Hydrogen Energy* **43**, 9558–9568 (2018).
36. Sadhukhan, A. K., Gupta, P. & Saha, R. K. Modelling and experimental studies on pyrolysis of biomass particles. *J. Anal. Appl. Pyrol.* **81**, 183–192 (2008).
37. Sharma, P. & Sharma, A. K. Application of response surface methodology for optimization of fuel injection parameters of a dual fuel engine fuelled with producer gas-biodiesel blends. *Energy Sources A Recov. Utiliz. Environ. Effects* **00**, 1–18 (2021).
38. Sharma, P. Prediction-optimization of the effects of di-tert butyl peroxide-biodiesel blends on engine performance and emissions using multi-objective response surface methodology. *J. Energy Resour. Technol. Trans. ASME* **144**, 1–26 (2022).
39. Sharma, P. & Sharma, A. K. AI-based prognostic modeling and performance optimization of CI engine using biodiesel-diesel blends. *Int. J. Renew. Energy Resour.* **11**, 701–708 (2021).
40. Sharma, P. & Sahoo, B. B. An ANFIS-RSM based modeling and multi-objective optimization of syngas powered dual-fuel engine. *Int. J. Hydrogen Energy* **47**, 19298–19318 (2022).
41. Hemmat Esfe, M. & Sadati Tilebon, S. M. Statistical and artificial based optimization on thermo-physical properties of an oil based hybrid nanofluid using NSGA-II and RSM. *Physica A* **537**, 122126 (2020).
42. Das, S. & Goud, V. V. RSM-optimised slow pyrolysis of rice husk for bio-oil production and its upgradation. *Energy* **225**, 120161 (2021).
43. Tripathi, M., Bhatnagar, A., Mubarak, N. M., Sahu, J. N. & Ganesan, P. RSM optimization of microwave pyrolysis parameters to produce OPS char with high yield and large BET surface area. *Fuel* **277**, 118184 (2020).
44. Jha, K. K., Kannan, T. T. M., Chandradass, J., Wilson, D. V. H. & Das, A. Analysis and simulation of mini pyrolysis reactor for conversion of plastic waste into fuel. *Mater. Today Proc.* https://doi.org/10.1016/j.matpr.2021.02.408 (2021).

## Author contributions

All authors equally contributed to conceptualization, writing, testing, results etc.

## Competing interests

The authors declare no competing interests.

## Additional information

**Publisher's note** Springer Nature remains neutral with regard to jurisdictional claims in published maps and institutional affiliations.